Journal of Catalysis **190,** 118–127 (2000)
doi:10.1006/jcat.1999.2732, available online at http://www.idealibrary.com on IDEAL®

Partial Oxidation of Methane on Silica-Supported Silicomolybdic Acid Catalysts in an Excess Amount of Water Vapor

Tomomi Sugino,* Ayako Kido,* Naoto Azuma,* Akifumi Ueno,*[,1] and Yasuo Udagawa†

*Department of Materials Science, Faculty of Engineering, Shizuoka University, 3-5-1 Johoku, Hamamatsu 432-8561, Japan; and †Research Institute for Scientific Measurements, Tohoku University, 2-1-1 Katahira, Aoba, Sendai 980-8577, Japan
E-mail: tcaueno@eng.shizuoka.ac.jp

Received July 5, 1999; revised October 11, 1999; accepted October 13, 1999

Partial oxidation of methane into oxygenates such as methanol and formaldehyde on highly dispersed MoO_3/SiO_2 catalysts was studied in an excess amount of water vapor. The reaction was carried out at 873 K using gases consisting of oxygen, methane, and water vapor. The selectivity of oxygenates was found to be a strong function of water vapor, and increased as the fraction of water vapor in a feed gas increased. Inversely, the selectivity of CO and CO_2 in the products decreased as the fraction of water vapor increased. This is ascribed to the formation of silicomolybdic acid (SMA: $H_4SiMo_{12}O_{40}$) over the silica surface during the reaction, partially evidenced by IR measurements. Accordingly, silica-supported SMA catalysts were prepared and applied to the partial oxidation of methane under the same conditions as described above to see if SMA works as the active species for the reaction. Although SMA easily decomposed into SiO_2 and MoO_3 at 873 K without water vapor, it worked well for the production of oxygenates when the fraction of water vapor was more than 50% in the feed gas. The yield of oxygenates increased up to 20% of methane as the fraction of water vapor was around 60%; methane conversion was about 25% and the selectivity of oxygenates was 90%. In this paper, the authors will emphasize that SMA formed on the silica surface are the active species of silica-supported MoO_3 catalysts for the partial oxidation of methane in an excess amount of water vapor.

Key Words: **partial oxidation; methane; formaldehyde; silicomolybdic acid; water vapor.**

INTRODUCTION

Direct conversion of methane into oxygenates such as methanol and formaldehyde has been of significant interest in the field of chemical engineering and catalysis for decades (1). There have been, at least, two problems in this research program. One is the design of a reactor that is effective enough to depress the successive oxidation of methanol and formaldehyde produced. The other is devising catalysts that work well for the selective production of oxygenates. A key point in the first problem is the residence time of oxygenates produced on catalysts (2). Since catalysts employed for the reaction generally work well at temperatures higher than 873 K, the oxygenates still remaining on the catalyst surface are further oxidized into CO and CO_2 (3). While for the latter problem, specification of the active sites formed on the catalyst surface is important since it was reported that methane adsorbed on one site of the catalyst preferentially produced CO_2 and methane adsorbed on the other sites was favorable to the production of oxygenates (4). In the present work we have tried to see if SMA formed on the silica surface is the active species for the production of oxygenates from methane.

Most of the work published before 1986 is appraised in a review by Pitcher and Klier (5), where molybdenum oxide-based catalysts were reported to be one of the most promising catalysts for the partial oxidation of methane. Many papers have been published on the structures of surface molybdates formed on the silica-supported molybdenum oxide catalysts (6–10), but the conclusions are complicated and controversial. This is partially because of the variety of electronic states of molybdenum ions depending upon the preparation conditions employed, and it is partially due to the variety of polymolybdates depending upon the concentration of molybdenum oxide on catalysts.

Recently, it has been reported that molybdenum oxides reacted with silica support in ambient moisture to yield acidic molybdates containing silicon ions, silicomolybdic acid (SMA) (11–16). Though the generation of silicomolybdate mixed with polymolybdate was reported earlier by Castellan *et al.* (17), Gajardo *et al.* (18, 19) were the first to show that the silicomolybdate formed possessed acid properties by acidmetric titration. Papers concerning the catalytic performance of SMA for various reactions were reviewed by Misono (20) and by Kozhevnikov (21), but most of the works reviewed were done at lower temperatures because of the low thermal stability of SMA. It is well accepted that SMA decomposes into SiO_2 and MoO_3 when it is calcined at temperatures higher than 573 K (22). The

---

[1] To whom all correspondence should be addressed.

0021-9517/00 $35.00

thermal stability of SMA was found to be improved by supporting on the silica surface, where the SMA still remained on calcination at 773 K (23). However, the partial oxidation of methane has been carried out in the temperatures range 723–923 K because of the extremely low reaction rate (24), and SMA supported or generated on silica was decomposed into MoO_3 crystallites during the reaction (15, 25, 26). Accordingly, nothing has been reported on the catalytic performances of actual SMA for the partial oxidation of methane at the higher temperatures.

Since SMA or analogous species are generated on silica according to the reaction $SiO_2 + 12MoO_3 + 2H_2O = H_4SiMo_{12}O_{40}$, the present authors have conceived that they might be stable even at higher temperatures, if sufficient amounts of water vapor are continuously supplied to the silica-supported MoO_3 or SMA catalysts. The results obtained will be discussed below.

EXPERIMENTAL

1. *Preparation of Silica-Supported MoO_3 Catalysts*

Silica-supported MoO_3 catalysts were prepared by two different methods, impregnation and sol/gel methods. Impregnation was carried out using an aqueous solution of $(NH_4)_6Mo_7O_{24}4H_2O$ and silica powder, prepared by hydrolysis of ethylsilicate. In the sol/gel method (27, 28) $(NH_4)_6Mo_7O_{24}4H_2O$ dissolved in ethylene glycol was added into ethylsilicate to be hydrolyzed into gels. Both catalysts were dried at 383 K for 24 h, followed by calcination at 873 K for 2 h, and 1.5 g of the catalysts was submitted to the reaction. The amount of MoO_3 loaded was 2 wt% of the catalysts, since low concentrations of MoO_3 generally lead to higher dispersions of Mo ions in the catalysts (15, 24).

2. *Preparation of Silica-Supported SMA Catalysts*

Silica-supported SMA catalysts were prepared by impregnation using an aqueous solution of 12-molybdosililic acid and silica powder. Silica powders were prepared by hydrolysis of ethylsilicate at pH 2, followed by calcination at 873 K for 2 h, and the specific surface area of the silica prepared was 570 m^2/g. The impregnated catalyst was dried at 393 K for 24 h, and 1.5 g of the dried catalyst was submitted to the reaction without further calcination because of the poor thermal stability (22). SMA loading was varied from 6 to 36 wt% of the catalysts.

3. *Characterization of Catalysts*

Since no XRD signals were detected for silica-supported MoO_3 catalysts, extended X-ray absorption fine structure (EXAFS) was applied to see the structures around Mo ions in the catalysts; the details of the EXAFS measurements have been noted elsewhere (29). The formation of SMA on silica-supported MoO_3 catalysts during the reaction at 873 K in the presence of an excess amount of water vapor was identified by diffuse reflectance IR spectroscopy (Shimadzu, FTIR-8200). IR measurements were carried out at room temperature throughout the work. The decomposition behavior of SMA in silica-supported SMA catalysts was also monitored by IR measurements. The catalyst was calcined at elevated temperatures for 2 h in dry flowing nitrogen, and the IR measurements were carried out at room temperature. The transmission electron microscope (TEM, Hitachi-H800) was operated at an accelerating voltage of 200 kV in order to observe MoO_3 crystallites dispersed in the silica-supported MoO_3 catalysts; details of the TEM measurements have also been described in the previous paper (30).

4. *Activity Measurements for Partial Oxidation of Methane*

The partial oxidation of methane was carried out using a flow reactor, as shown in Fig. 1, made of stainless steel. In the middle of the reactor 1.5 g of the catalyst powder was placed, and the gases consisting of CH_4, O_2, and water vapor were conducted from the top of the reactor through a mixing tube. Glass beads (5 mm ϕ) were packed in the mixing tube in order to achieve homogeneous mixing of the gases. Water was supplied from a pump (GL Science, NTD-006MG) and vaporized in the mixing tube, heated at 523 K. All tubes, made of stainless steel, were heated at 523 K in order to prevent deposition of water on the tube wall. The flow rate of the dry gas (CH_4/O_2) was always 2.0 L/h, though the CH_4/O_2 volume ratio was varied from 9/1 to 4/6; generally the ratio was 9/1. The flow rate of

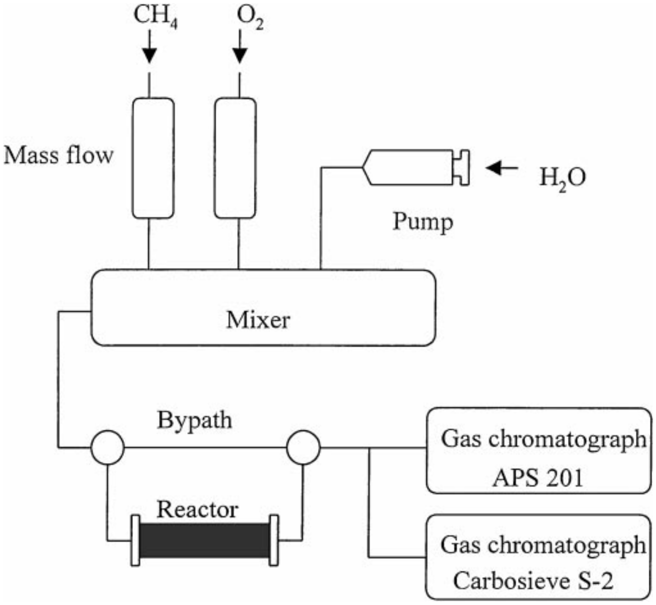

FIG. 1. Apparatus employed for partial oxidation of methane.

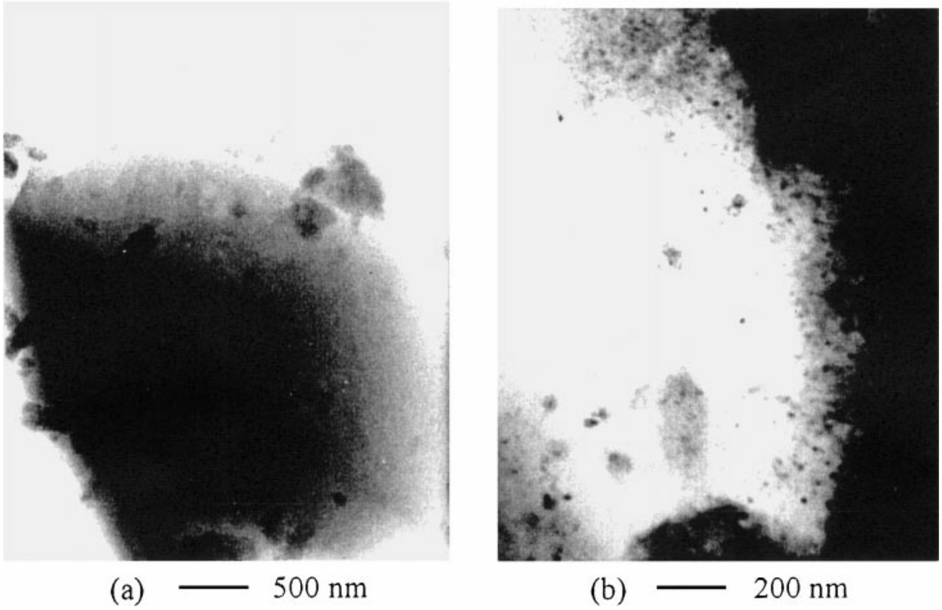

FIG. 2. TEM photographs of (a) impregnated and (b) sol/gel catalysts.

water vapor at STP was also varied from 0.5 to 3.5 L/h with a constant flow rate of the CH_4/O_2 mixture, 2.0 L/h.

The gases passed through the catalyst bed were analyzed with two gas chromatographs; one was for the analysis of CH_4, CO, and CO_2 using a column packed with Carbosieve S-II, and the other was for the analysis of methanol, formaldehyde, and water vapor using an ASP-201 column. The sampling gases were directly introduced into the gas chromatographs using a six-way valve equipped with a 0.5-ml gas sampling tube, which was heated at 523 K in order to avoid condensation of water vapor on the wall of the sampling tube. The concentration of O_2 could not be precisely measured due to leaked air on gas sampling. The amount of formaldehyde produced was also measured by conventional chemical analysis using a trap filled with aqueous solution of Na_2SO_3 and a certain amount of H_2SO_4 (31). Formaldehyde produced reacts with Na_2SO_3 as follows, and the NaOH formed was consumed by H_2SO_4 so that the reaction always proceeded to the right. Finally, the H_2SO_4 still remaining in the solution could be measured by titration using a standard NaOH aqueous solution:

$$HCHO + Na_2SO_3 + H_2O \rightarrow HCH(OH)SO_3Na + NaOH.$$

RESULTS AND DISCUSSION

1. MoO_3 Dispersion in the Silica-Supported MoO_3 Catalysts

A significant difference in the dispersion of MoO_3 crystallites was observed in two kinds of silica-supported MoO_3 catalysts. MoO_3 crystallites dispersed in the catalyst prepared by sol/gel method were 2 ∼ 3 nm, while those dispersed in the catalyst by the impregnation method were 200 ∼ 300 nm, estimated from the photographs shown in Fig. 2. According to the previous paper, metal ions dissolved in ethylene glycol form cyclic metal glycoxides (Scheme 1, part 1), which then react with ethylsilicate to form the –O–Si–O–M–O–Si–O– structure (Scheme 1, part 2) as shown in Scheme 1.

The structure (2) expands into gels during hydrolysis of the sol/gel method, and metal ions are separately trapped in the –O–Si–O– network of the dried silica gels (27, 28). Some of the trapped metal ions migrate from the network and coagulate to form finely divided metal oxide crystallites, when the dried gels are calcined at higher temperatures. The difference in the MoO_3 dispersion in these silica-supported MoO_3 catalysts is also confirmed by EXAFS measurements,

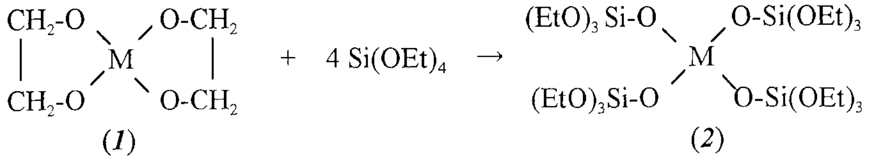

SCHEME 1

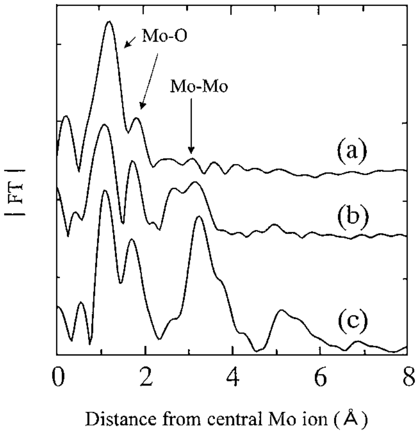

FIG. 3. EXAFS Fourier spectra of (a) sol/gel and (b) impregnated catalysts, and (c) standard MoO$_3$ crystallites.

as given in Fig. 3, where EXAFS Fourier spectra of the calcined MoO$_3$/SiO$_2$ catalysts, prepared by the impregnation and sol/gel methods, and standard MoO$_3$ crystallites are shown. Three peaks were observed for the standard MoO$_3$ crystallites at the distances of 1.25, 1.85, and 3.25 Å from a central Mo atom (phase shift uncorrected). The Mo atom is located in the distorted octahedron of MoO$_3$, and the oxygen atoms bound to Mo ions can be classified into two groups, four oxygen atoms with shorter distances (average 1.82 Å) and two oxygen atoms with longer distances (average 2.30 Å) (33). Hence, the first two peaks observed at 1.25 and 1.85 Å are assigned to Mo–O bonds, and the peak observed at 3.25 Å corresponds to the Mo–Mo bond in MoO$_3$ crystallites (8, 34). The EXAFS Fourier pattern of the impregnated catalyst was almost the same as that of standard MoO$_3$ crystallites, suggesting the formation of bulk-like MoO$_3$ crystallites in the impregnated catalyst. While the EXAFS Fourier pattern of the sol/gel catalyst was much different from those of standard MoO$_3$ crystallites and of the impregnated catalyst, the relative intensity of the second peak is much reduced and the third peak is almost nonexistent. This indicates the loss of the long-distance ordering around Mo atoms, and hence the formation of finely divided MoO$_3$ crystallites in the sol/gel catalysts is suggested (35, 36). The difference in the MoO$_3$ dispersion in impregnated and sol/gel catalysts is believed to be the origin of the differences in the catalytic activity for partial oxidation of methane, as given in Table 1.

As can be seen in Table 1, both the methane conversion and the selectivity of oxygenates (methanol and formaldehyde) on the sol/gel catalysts were much higher than those on the impregnated catalysts at any temperature employed.

2. *Formation of Silicomolybdic Acid (SMA) on the Sol/Gel Catalysts*

The reason the sol/gel catalysts exhibited higher activity and selectivity than the impregnated catalysts was studied. Figure 4 shows IR spectra for both catalysts, fresh and used for partial oxidation of methane at 873 K for 6 h in the presence of an excess amount of water vapor. The IR spectra of the fresh and used impregnated catalysts were the same and showed an absorption peak at 975 cm^{-1}, characteristic of the terminal Mo=O bond of distorted polymolybrate ions such as Mo$_7$O$_{24}$ and Mo$_8$O$_{26}$ (25, 37, 38). Wachs *et al.* are of the opinion that these polymolybdate ions are isolated, or monomeric, on the silica surface when Mo loading is less than 2 wt% of the catalysts (37, 38). However, the data obtained in the present work by TEM and EXAFS revealed the presence of small MoO$_3$ crystallites, instead of the isolated polymolybdate ions, on the silica surface. This was due to the difference in the calcination temperature; 773 K for the work done by Wachs *et al.* and 873 K for the present work. The isolated polymolybdate ions were, probably, coagulated into distorted MoO$_3$ crystallites on calcination at 873 K.

TABLE 1

Activities of MoO$_3$/SiO$_2$ Catalysts Prepared by the Impregnation and Sol/Gel Methods for Partial Oxidation of Methane in an Excess Amount of Water Vapor

Catalyst	Temperature (K)	CH$_4$ conv. (%)	Selectivity (%)				Yields (%)
			HCHO	CH$_3$OH	CO	CO$_2$	CH$_3$OH + HCHO
Impreg.	773	0.58	32	2	25	41	0.20
	823	1.2	13	1	35	51	0.17
	873	4.0	12	1	33	54	0.52
	923	6.6	1	0	18	81	0.07
Sol/gel	773	1.0	73	13	0	14	0.86
	823	2.9	52	8	10	30	1.7
	873	8.2	35	11	17	37	3.8
	923	12.0	11	4	23	62	1.8

Note. The flow rates of CH$_4$, O$_2$, and water vapor were 1.8, 0.2, and 2.0 L/h, respectively, and the amount of catalyst employed was 1.5 g in all experimental runs.

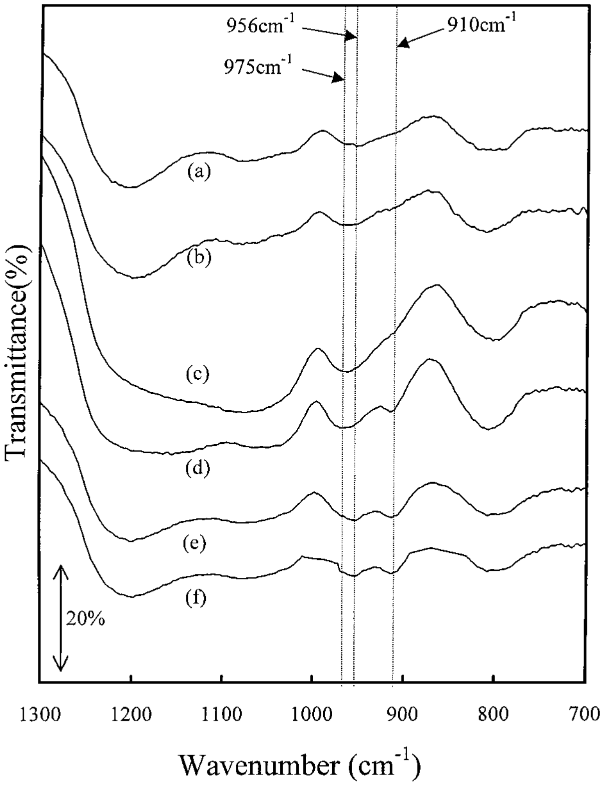

FIG. 4. IR spectra of the impregnated catalyst (a) before and (b) after the reaction, and the sol/gel catalyst (c) before and (d) after the reaction. IR spectra (e) and (f) are for 12SMA/SiO_2 catalyst before and after the reaction at 873 K, respectively.

Accordingly, no difference in the IR spectra before and after the reaction indicates that distorted MoO_3 in the impregnated catalysts still remained even after the reaction at 873 K for 6 h.

In contrast, the used sol/gel catalysts showed two peaks at 975 and 910 cm^{-1}, though the fresh one showed a single peak at 975 cm^{-1}. The peak at 910 cm^{-1} has been assigned to the Si–O–Mo bond of SMA crystallites (15, 25), which should be accompanied by the peak at 956 cm^{-1} due to the terminal Mo=O bond of SMA crystallites (see spectrum (e)). But the peak at 956 cm^{-1} was, probably, overlapped with the peak at 975 cm^{-1} assigned to the terminal Mo=O bond of the distorted MoO_3 crystallites, coexisting in the catalyst. Thus, it was concluded that SMA, as well as the distorted MoO_3 crystallites, was formed in sol/gel catalysts during the reaction at 873 K in an excess of water vapor. SMA formation by the solid-state reaction of MoO_3 and SiO_2 in the presence of water vapor has been reported as follows (11–19, 25):

$$SiO_2 + 12MoO_3 + 2H_2O = H_4SiMo_{12}O_{40}.$$

Consequently, the difference in MoO_3/SiO_2 catalysts prepared by impregnation and the sol/gel method is in the formation of SMA during partial oxidation of methane in the presence of an excess amount of water vapor. The solid-state reaction shown above was likely enhanced in the sol/gel catalysts because of the high dispersion of MoO_3 crystallites in silica. This leads us to the speculation that SMA might be the active species for partial oxidation of methane into oxygenates, although Deltcheff *et al.* (14, 15) have reported that trimolybdic groups, interacted with silica support through Si–O–Mo bonds, were the active species for the partial oxidation of methanol at 523 K.

Looking back to the results given in Table 1, the selectivity of CO and CO_2 on the impregnated catalysts was much higher than that on the sol/gel catalysts. It is common to explain that the methanol and formaldehyde yielded are further oxidized into CO and CO_2 on the impregnated catalysts, where MoO_3 crystallites are predominant on the silica surface. Another possible explanation is that the direct oxidation of methane into CO and CO_2 preferentially proceeds on the distorted MoO_3 crystallites, as well as the subsequent oxidation of methanol and formaldehyde. Banares *et al.* (16, 25) are also of the opinion that CO_2 originates directly from methane rather than from further oxidation of methanol and formaldehyde. Spencer reported a simplified reaction scheme for partial oxidation of methane on MoO_3/SiO_2 and suggested a direct production of CO_2 from methane (39). The reason the selectivity of CO and CO_2 was low on the sol/gel catalysts seems to be attributed to the smaller amounts of MoO_3 crystallites in sol/gel catalysts under the working conditions, i.e., SMA are the dominant species in sol/gel catalysts. Hence, the low selectivity of CO and CO_2 and the high selectivity of formaldehyde were achieved on the sol/gel catalysts.

3. *Thermal Stability of SMA Supported on Silica*

The thermal stability of bare SMA was studied by IR spectroscopy and was compared with that of SMA supported on silica. Figure 5A shows the IR spectra of bare SMA at the elevated temperatures. Two absorption peaks characteristic of SMA were observed at 956 and 910 cm^{-1}, assigned to the terminal Mo=O and Mo–O–Si, respectively. These peaks decreased with the elevation of calcination temperature, and diminished at the temperatures higher than 673 K. The absorption peak observed at 997 cm^{-1} was assigned to the terminal M=O of MoO_3 crystallites, and the small amounts of MoO_3 were found to be contaminated in the bare SMA. The peak at 997 cm^{-1} increased, and new peaks were observed at 820 and 1050 cm^{-1}, assigned to the symmetric and asymmetric stretching vibrations of the Si–O–Si bond in silica, when SMA was calcined at temperatures higher than 673 K. These results indicate that SMA decomposed into MoO_3 and SiO_2 in dry nitrogen flowing at 673 K or higher temperatures.

Figure 5B shows the IR spectra of SMA in 27 wt% SMA/SiO_2 catalyst (abbreviated as 27SMA/SiO_2 below)

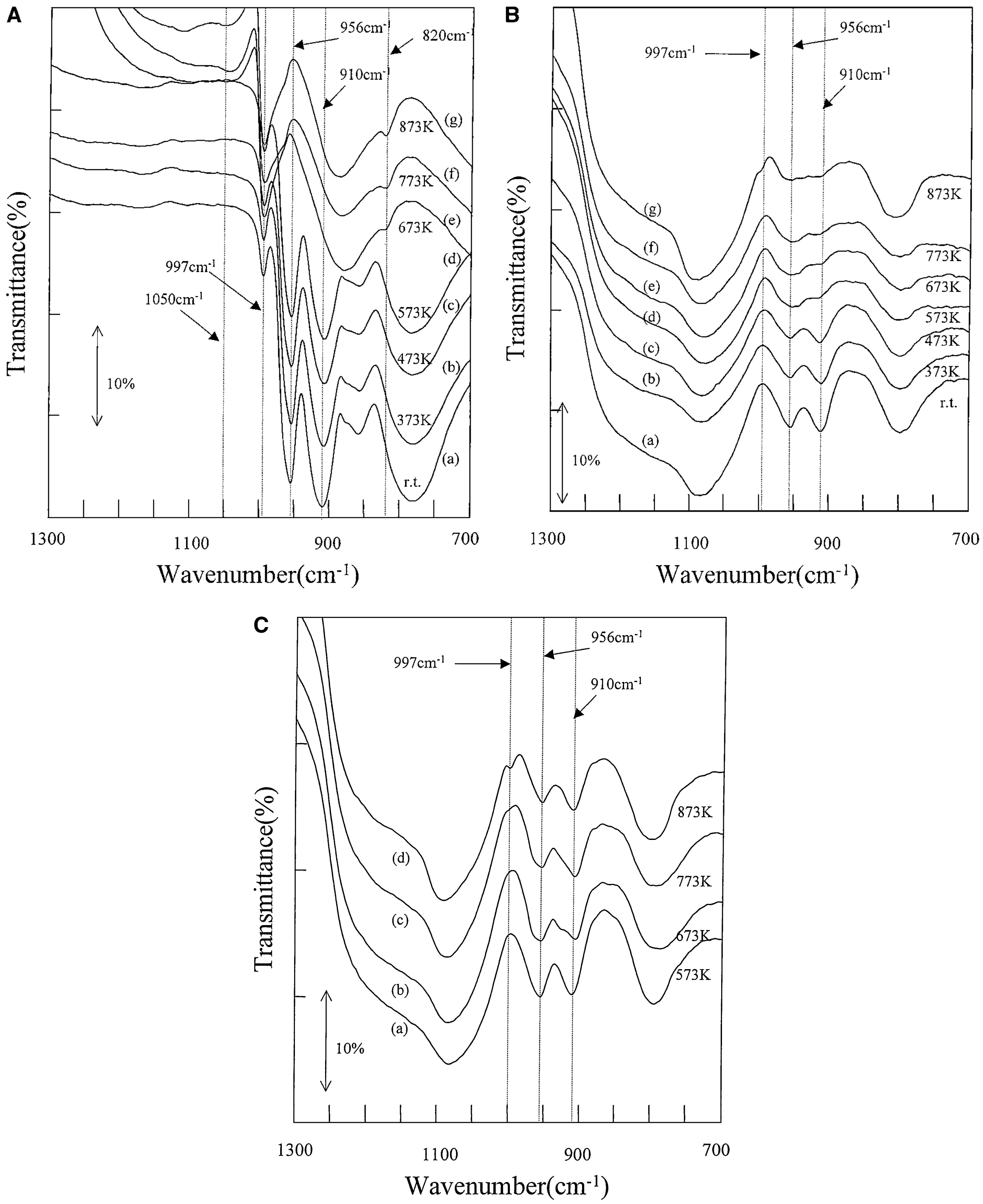

FIG. 5. (A) IR spectra of bare SMA: (a) at room temperature, and calcined for 2 h (b) at 373 K, (c) at 473 K, (d) at 573 K, (e) at 673 K, (f) at 773 K, and (g) at 873 K. (B) IR spectra of 27SMA/SiO$_2$: (a) at room temperature, and calcined for 2 h (b) at 373 K, (c) at 473 K, (d) at 573 K, (e) at 673 K, (f) at 773 K, and (g) at 873 K. (C) IR spectra of 27SMA/SiO$_2$ exposed to water vapor at room temperature for 24 h after being heated for 2 h (a) at 573 K, (b) at 673 K, (c) at 773 K, and (d) at 873 K.

at elevated temperatures. Two peaks were detected at 956 and 910 cm^{-1}, which are characteristic of SMA, and these two peaks decreased when the calcination temperature increased. However, trace amounts of absorption were still detected even after the catalyst was calcined at 873 K for 2 h, though a peak assigned to the terminal Mo=O of MoO_3 appeared at 997 cm^{-1}. This indicates that SMA in the silica-supported catalyst is more thermally stable than bare SMA (23). It would be interesting to show that the decomposed SMA in the silica-supported catalyst was recovered by exposure to water vapor at room temperature. Figure 5C shows the IR spectra of SMA recovered by exposing to the saturated water vapor at room temperature for 24 h. Even for the catalysts calcined at 873 K for 2 h, SMA in the catalysts was almost regenerated by exposure to water vapor. This suggests that MoO_3 produced by the decomposition of silica-supported SMA is highly dispersed in the SiO_2 support as finely divided crystallites. The spectra designated as (e) and (f) in Fig. 4 are the spectra of the fresh 12SMA/SiO_2 catalyst and of that used for the reaction at 873 K in an excess of water vapor for 24 h, respectively. Both spectra show two absorption peaks at 956 and 910 cm^{-1}, suggesting the presence of SMA during methane oxidation at 873 K. In other words, decomposition of SMA into MoO_3 and SiO_2 during the reaction was strongly suppressed in an excess amount of water vapor.

4. *Catalytic Activity of Silica-Supported SMA Catalysts*

4.1. Effects of water vapor upon the catalytic activity. Figure 6 shows the effects of water vapor upon the catalytic activity of 27 wt% SMA/SiO_2 for partial oxidation of methane at 873 K using gases consisting of CH_4 (1.2 L/h) and O_2 (0.8 L/h). Since the specific surface area of the silica support used was 570 m^2/g, monolayer coverage of SMA on the silica surface was achieved with 27SMA/SiO_2, assuming the diameter of a SMA molecule to be 25 Å. It was found that the methane conversion increased as the fraction of water vapor in the feed gas increased up to 2 L/h, corresponding to 50% water vapor in the feed. Even when the fraction of water vapor was increased further, the methane conversion remained 20 ∼ 25% with around 90% selectivity of oxygenates (methanol and formaldehyde). Because of the significant amount of formaldehyde produced, it was hard to distinguish the peak due to methanol from the peak due to formaldehyde in our GC column. Hence, instead of the individual selectivity of methanol and formaldehyde, the selectivity of oxygenates (including both methanol and formaldehyde) was used in this paper. However, most of the oxygenates produced in the present work were formaldehyde, and the amount of methanol in the oxygenates was estimated to be around 5% of the oxygenates at high methane conversions.

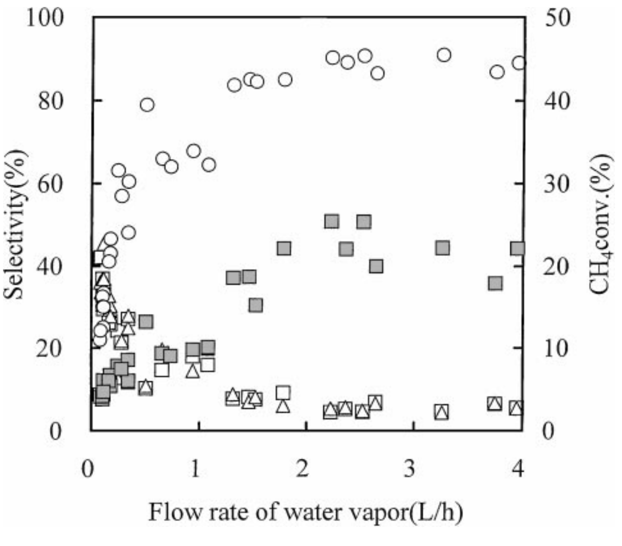

FIG. 6. Change in the catalytic activity of 27SMA/SiO_2 at 873 K with the fraction of water vapor in the feed gas, consisting of CH_4 (1.2 L/h) and O_2 (0.8 L/h): ○, oxygenates; □, CO; △, CO_2 selectivity; □, CH_4 conversion.

The selectivity of oxygenates increased as the fraction of water vapor increased up to 50% in the feed, and, inversely, the selectivity of CO and CO_2 decreased. Since CO and CO_2 might be produced on MoO_3 crystallites in the catalysts, as discussed above, most of Mo ions remained as SMA on the silica support when the fraction of water vapor was higher than 50% (2 L/h) in the feed. As the fraction decreased to lower than 50%, CO and CO_2 selectivity increased, suggesting the deposition of MoO_3 crystallites in the catalysts by the decomposition of SMA as follows:

$$H_4SiMo_{12}O_{40} \rightarrow SiO_2 + 12MoO_3 + 2H_2O.$$

Consequently, one of the most important roles of the water vapor is to suppress the decomposition of SMA into SiO_2 and MoO_3 crystallites, and around 50% water vapor in the feed gas is necessary to stabilize SMA crystallites on the silica surface at 873 K. The yield of oxygenates was as high as 20% methane when the fraction of water vapor was higher than 50% in the feed. The selectivities of CO and CO_2 were as low as 5% each, and this was attributed to the suppression of SMA decomposition into MoO_3 crystallites, where further oxidation of oxygenates and, probably, the direct oxidation of methane into CO and CO_2 seem to be enhanced.

4.2. Effects of methane/oxygen ratio upon the catalytic activity. The stoichiometric ratios of methane to oxygen in the partial oxidation of methane into methanol and formaldehyde are 2 and 1, respectively. However, in most of the work the methane/oxygen ratio employed was 9 in order to suppress CO_2 formation. In the present work, the effects of the CH_4/O_2 ratio upon the catalytic activity were studied in the presence of 60 vol% water vapor in the feed, 3 L/h water vapor and 2 L/h ($CH_4 + O_2$). The CH_4/O_2 ratio

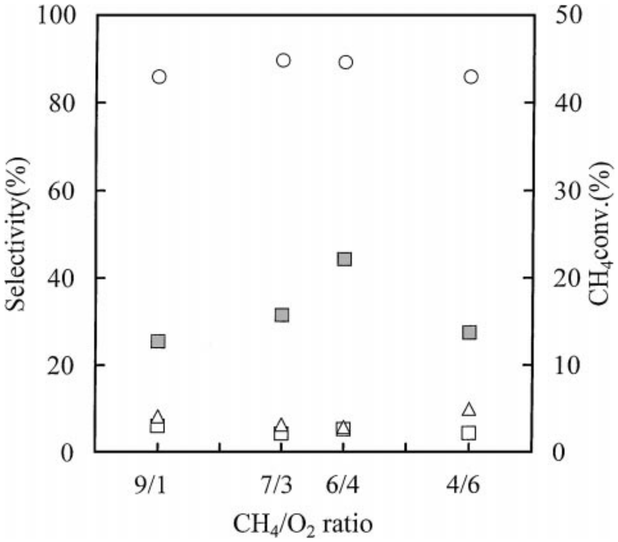

FIG. 7. Change in the catalytic activity of 27SMA/SiO$_2$ at 873 K with the CH$_4$/O$_2$ ratio in the feed gas. The total flow rate of CH$_4$/O$_2$ was 2 L/h and that of water vapor was kept at 3 L/h: ○, oxygenates; □, CO; △, CO$_2$ selectivity; □, CH$_4$ conversion.

was varied from 9/1 to 4/6 using 1.5 g 27SMA/SiO$_2$ catalyst at 873 K. The results given in Fig. 7 show that the methane conversion increased to higher than 20% when the CH$_4$/O$_2$ ratio decreased to 6/4, though the selectivity of oxygenates was constant, 85–90%. Hence, the yield of oxygenates increased with a decrease in CH$_4$/O$_2$ ratio to 6/4. However, the yield of oxygenates decreased when the CH$_4$/O$_2$ ratio was 4/6. This is partially due to a decrease in the methane conversion and partially due to an increase in the CO$_2$ selectivity by further oxidation of oxygenates. Consequently, the optimum CH$_4$/O$_2$ ratio for the production of oxygenates was 6/4 under the present reaction conditions. Generally, the selectivity of CO and CO$_2$ increased as the methane conversion increased during partial oxidation of methane, and the results obtained in this work might be very specific.

It must be mentioned that oxygen is inevitable for this reaction because one may imagine the production of oxygenates through CO and H$_2$, yielded by steam reforming of methane, as $CH_4 + H_2O \rightarrow CO + 3H_2$. However, the yield of oxygenates was less than 0.2% of the methane employed when no oxygen was added into the feed at 873 K; i.e., the feed gas is the mixture of CH$_4$ and an excess amount of H$_2$O.

4.3. Effects of SMA loading upon the catalytic activity. Since the reaction takes place on the SMA surface, methane conversion was expected to increase with an increase in the SMA loading on silica. The effects of SMA loading upon the catalytic activity were studied at 873 K using gases consisting of CH$_4$ and O$_2$ with the CH$_4$/O$_2$ ratio being 9/1. The gas flow rate was settled to be 2.0 L/h and the amount of water vapor added was 3.0 L/h, corresponding 60 vol% water vapor in the feed. Figure 8 shows that the methane conversion increased with an increase in the SMA loading on the catalysts, while the selectivity of oxygenates was almost constant regardless of the loading. Hence, the yield of oxygenates increased as the SMA loading increased up to 27 wt%, but no further increase in the yield was observed when the SMA loading was higher than 27 wt% of the catalysts. SMA monolayer coverage will be achieved over the silica surface (540 m^2/g) with 27 wt% loading, based on the assumption that an SMA molecule is 25 Å in diameter. This indicates that only the first layer of SMA works well for the partial oxidation of methane into formaldehyde, but SMA located at the second layer does not. Similar results have been reported for the dehydration of *t*-butyl alcohol into isobutene on silica-supported phosphomolybdic acid (HPM; $H_3PMo_{12}O_{40}$) catalyst (40, 41). According to these papers, only the first layer of HPM was effective for the gas-phase dehydration of *t*-butyl alcohol, but for the liquid phase reaction a few layers of HPM took part in the dehydration reaction through a pseudo-liquid mechanism (20).

Since one of the features of silica-supported SMA is the presence of acid sites (H$^+$) widely distributed on the catalyst surface, H$^+$ may play an important role for the partial oxidation of methane into formaldehyde. It has been reported that protons (H$^+$) in the solid superacid, consisting of Cr^{3+}–Zr^{4+}–SO$_4$/SiO$_2$, attacked methane to produce CH_5^+ as an intermediate to oxygenates such as methanol and formaldehyde (42). Olah *et al.* were the first to propose the generation of pentacoordinated carbocations (CH_5^+) during the ionization of methane in the presence of superacid (SbF$_5$/HSO$_3$F) at 353–423 K (43). Their work was extended to the direct production of methanol from methane in the presence of the superacid, but hydrogen peroxide was

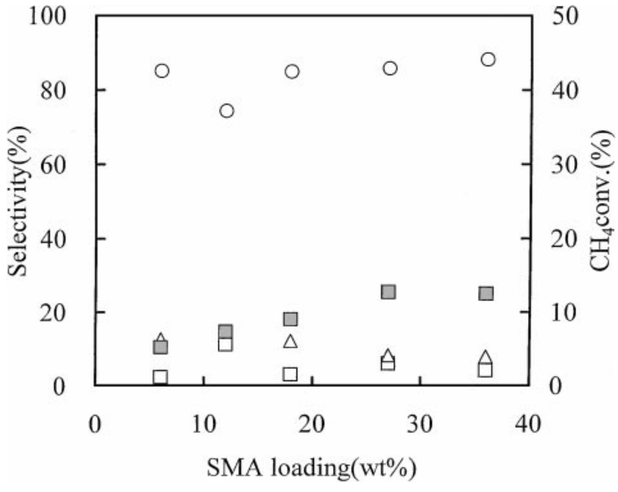

FIG. 8. Change in the catalytic activity of SMA/SiO$_2$ with SMA loading. The reaction was carried out at 873 K using CH$_4$/O$_2$ (9/1 volume ratio) and water vapor (60 vol% in the feed). ○, oxygenates; □, CO; △, CO$_2$ selectivity; □, CH$_4$ conversion.

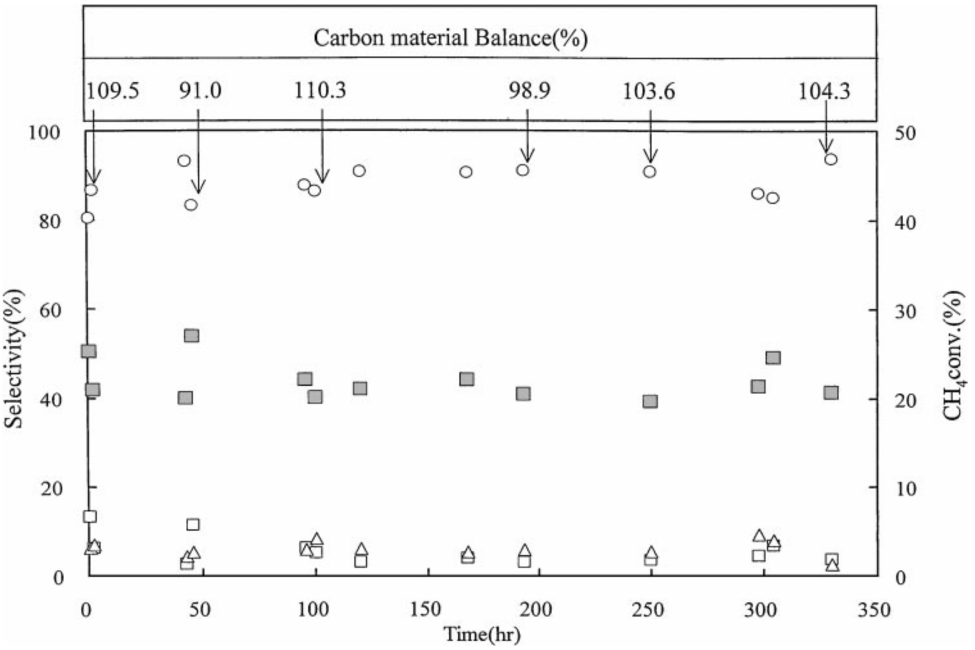

FIG. 9. Durability test of 27SMA/SiO$_2$ at 873 K and the carbon mass balance. The reaction was carried out at 873 K using CH$_4$/O$_2$ (6/4 volume ratio) and water vapor (60 vol% in the feed): ○, oxygenates; □, CO; △, CO$_2$ selectivity; □, CH$_4$ conversion.

necessary for the production of methanol (44). We are not sure if carbocations such as CH_5^+ are generated, or not, on the SMA surface, but we believe that interactions between CH$_4$ and H$^+$ on SMA promote the partial oxidation of methane into oxygenates. Methane directly adsorbed on MoO$_3$ crystallites, deposited by the decomposition of SMA, likely leads to CO$_2$ production.

4.4. Durability tests of silica-supported SMA catalysts. Finally, the durability of 27SMA/SiO$_2$ (1.5 g) was evaluated at 873 K for 350 h in the presence of 60 vol% water vapor in the feed gas, consisting of CH$_4$ and O$_2$ with a volume ratio of 6/4. The space velocity in the dry base was 1,400 h^{-1} and in the wet base it was 3,500 h^{-1}, since the gas flow rate employed was 2 L/h for the CH$_4$/O$_2$ mixture and 3 L/h for water vapor. The amounts of formaldehyde formed were analyzed by gas chromatography and, occasionally, by a titration using a standard NaOH solution, and the mass balance concerning carbon atoms was estimated using the following:

$$\sum(\mathrm{HCHO} + \mathrm{CO} + \mathrm{CO_2} + \text{unreacted } \mathrm{CH_4}) \\ \text{at the outlet}/\mathrm{CH_4} \text{ at the inlet.}$$

The results obtained are given in Fig. 9, suggesting a decrease in neither methane conversion nor oxygenate (formaldehyde) selectivity during a 350-h durability test. The methane conversion was 20–25% and the selectivity of oxygenates was constant around 90%, corresponding to a ca. 20% yield of oxygenates during the test. The mass balance deviated a little from 90 to 110%, measured by both gas chromatographs and chemical analysis. The amounts of formaldehyde measured by chemical analysis using aqueous solution of Na$_2$SO$_3$ were in good accordance with those measured by gas chromatographs. The deviation of mass balance mentioned above comes predominantly from the pulsation of the water supply.

CONCLUSION

The following conclusions were obtained in the present work:

1. MoO$_3$/SiO$_2$ catalysts with high dispersion of MoO$_3$ showed relatively high activity for the partial oxidation of methane into oxygenates in an excess amount of water vapor. This is due to the generation of SMA on the catalyst surface.
2. While the catalysts with low dispersion of MoO$_3$ showed poor activity, most of the methane reacted converted into CO and CO$_2$.
3. A high conversion of methane and a high selectivity of oxygenates (most of them are formaldehyde) were observed on silica-supported SMA catalysts with an excess amount of water vapor in the feed.
4. The role of the water vapor added was to suppress the thermal decomposition of SMA into MoO$_3$ and SiO$_2$ at higher temperatures.
5. Methane conversion increased with an increase in SMA loading until monolayer coverage of SMA on SiO$_2$

was achieved, while the selectivity of oxygenates was constant, ca. 90%.

6. An optimum CH_4/O_2 ratio in the feed was 6/4 for a higher yield of oxygenates.

7. A 350-h durability test of the 27SMA/SiO_2 catalyst at 873 K in an excess amount of water vapor showed no deactivation, 20–25% methane conversion, and ca. 90% selectivity of oxygenates, which corresponds to a ca. 20% yield of oxygenates.

REFERENCES

1. Wang, Y., and Otsuka, K., "Proceedings, 11th International Congress on Catalysis," A-35, p. 397. Elsevier, Amsterdam/New York, 1996.
2. Casey, P. S., McAllister, T., and Foger, K., *Ind. Eng. Chem. Res.* **33**, 1120 (1994).
3. Amiridis, M., Rekoske, J., Dumesic, J., and Rudd, D., AIChE **37**, 87 (1991).
4. Smith, M. R., and Ozkan, U. S., *J. Catal.* **141**, 124 (1993).
5. Pitcher, R., and Klier, K., *Catal. Rev.* **28**, 13 (1986).
6. Cornac, M., Janin, A., and Lavalley, J. C., *Polyhedron* **5**, 183 (1986).
7. Iwasawa, Y., *Adv. Catal.* **35**, 187 (1987).
8. Kakuta, N., Tohji, K., and Udagawa, Y., *J. Phys. Chem.* **92**, 8583 (1988).
9. Liu, T. C., Forissier, M., Coudurier, G., and Vedrine, J. C., *J. Chem. Soc. Faraday Trans. 1* **85**, 1607 (1989).
10. Desikan, A. N., Huang, L., and Oyama, S. T., *J. Phys. Chem.* **95**, 10050 (1991).
11. Rodrigo, L., Marcinkowska, K., Andot, A., Roberge, P., Kaliaguine, S., Stencel, J. M., Makovsky, L. E., and Diehl, J. R., *J. Phys. Chem.* **90**, 2690 (1986).
12. Stencel, J. M., Diehl, J. R., D'Este, J. R., Makovsky, L. E., Rodrigo, L., Marcinkowska, K., Andot, A., Roberge, P., and Kaliaguine, S., *J. Phys. Chem.* **90**, 4793 (1986).
13. Rodrigo, L., Andot, A., Roberge, P., and Kaliaguine, S., *J. Catal.* **105**, 175 (1987).
14. Tatibouet, J. M., Che, M., Amirouche, M., Fournier, M., and Deltcheff, C. R., *J. Chem. Soc. Chem. Commun.*, 1260 (1988).
15. Deltcheff, C. R., Amirouche, M., Che, M., Tatibouet, J. T., and Fournier, M., *J. Catal.* **125**, 292 (1990).
16. Banares, M. A., Fierro, J. F., and Moffat, J. B., *J. Catal.* **142**, 406 (1993).
17. Castellan, A., Bart, C. J., Vaghi, A., and Giordano, N., *J. Catal.* **42**, 162 (1976).
18. Gajardo, P., Grange, P., and Delmon, B., *J. Phys. Chem.* **83**, 1771 (1979).
19. Gajardo, P., Pirotte, D., Grange, P., and Delmon, B., *J. Phys. Chem.* **83**, 1780 (1979).
20. Misono, M., *Catal. Rev. Sci. Eng.* **29**, 269 (1987).
21. Kozhevnikov, I. V., *Catal. Rev. Sci. Eng.* **37**, 311 (1995).
22. Banares, M. A., Hu, H., and Waches, I. E., *J. Catal.* **150**, 407 (1994).
23. Kasztelan, S., Payen, E., and Moffat, J. B., *J. Catal.* **112**, 320 (1988).
24. Faraldos, M., Banares, M. A., Anderson, J. A., Hu, H., Waches, I. E., and Fierro, J. L., *J. Catal.* **160**, 214 (1996).
25. Banares, M. A., Hu, H., and Waches, I. E., *J. Catal.* **155**, 249 (1995).
26. Deltcheff, C. R., Aouissi, A., Bettahar, M. M., Launay, S., and Fournier, M., *J. Catal.* **164**, 16 (1996).
27. Ueno, A., Suzuki, H., and Kotera, Y., *J. Chem. Soc. Faraday Trans. 1* **79**, 127 (1983).
28. Tohji, K., Udagawa, Y., Tanabe, S., and Ueno, A., *J. Am. Chem. Soc.* **106**, 612 (1984).
29. Mizushima, T., Tohji, K., Udagawa, Y., and Ueno, A., *J. Am. Chem. Soc.* **112**, 7887 (1990).
30. Ishiguro, K., Ishikawa, T., Kakuta, N., Ueno, A., Mitarai, M., and Kamo, T., *J. Catal.* **123**, 523 (1990).
31. Siggia, S., and Maxcy, F., *Ind. Eng. Chem. Anal. Ed.* **19**, 1023 (1947).
32. Yoda, K., Kimoto, K., and Toda, T., *Kogyo Kagaku Zasshi* **67**, 909 (1064).
33. Kihlborg, L., *Ark. Kemi.* **21**, 357 (1963).
34. Clausen, B. S., Topsoe, H., Candia, R., Villadsen, J., Lengeler, B., Nielsen, J. A., and Christensen, F., *J. Phys. Chem.* **85**, 3868 (1981).
35. Greegor, R. B., Lytle, F. W., Chin, R. L., and Hercules, D. M., *J. Phys. Chem.* **85**, 1232 (1981).
36. Tohji, K., Udagawa, Y., Tanabe, S., Ida, T., and Ueno, A., *J. Am. Chem. Soc.* **106**, 5172 (1984).
37. Hardcastle, F. D., and Wachs, I. E., *J. Raman Spectrosc.* **21**, 683 (1990).
38. Hu, H., Wachs, I. E., and Bare, S. R., *J. Phys. Chem.* **95**, 10897 (1995).
39. Spencer, N. D., *J. Catal.* **109**, 187 (1988).
40. Ohtsuka, R., Morioka, Y., and Kobayashi, J., *Bull. Chem. Soc. Jpn.* **62**, 3195 (1989).
41. Ohtsuka, R., Morioka, Y., and Kobayashi, J., *Bull. Chem. Soc. Jpn.* **63**, 2071 (1990).
42. *Chem. Eng. News* Jan. 22, 21 (1990).
43. Olah, G. A., Klopman, G., and Schlosberg, R. H., *J. Am. Chem. Soc.* **91**, 3261 (1969).
44. Olah, G. A., Yoneda, N., and Parker, D. G., *J. Am. Chem. Soc.* **99**, 483 (1977).